2011 International Nuclear Atlantic Conference - INAC 2011
Belo Horizonte,MG, Brazil, October 24-28, 2011
ASSOCIAÇÃO BRASILEIRA DE ENERGIA NUCLEAR - ABEN
***ISBN:* 978-85-99141-04-5**

MCNP TO STUDY THE BF_3 DETECTION EFFICIENCY

Vinícius A. Castro[1], Tássio A. Cavalieri[1], Paulo T. D. Siqueira[1], Giuliana G. Fedorenko[1], Paulo R. P. Coelho[1] and Tufic M. Filho[1]

[1] Centro de Engenharia Nuclear – Instituto de Pesquisas Energéticas e Nucleares
Universidade de São Paulo
Avenida Lineu Prestes, 2242
05508-000 Cidade Universitária, SP
vcastro@ipen.br

ABSTRACT

One of the main parameters to monitor on the employment of the Boron Neutron Capture Therapy (BNCT) is the thermal neutron flux. It can be performed by different techniques such as the activation analysis and the detection by a Boron Trifluoride detector (BF_3). BF_3 detector is a real time neutron flux detector which retrieves results in real time. It is however necessary to study the efficiency of the BF_3 detectors when they are exposed to fields of different neutron energy spectra. BF_3 is known to have high efficiency for thermal neutrons (with energy up to 0.5 eV) due the presence of ^{10}B atoms in the detector. However, one must also understand how this detector interacts with other neutron energy ranges (epithermal and fast). This work shows the experiment and a set of associated simulations carried out in order to evaluate the BF_3 detector efficiency dependence on neutron energy spectra. A set of experiments was conducted in which a BF_3 detector was submitted to different mixed fields (field containing gamma rays and neutrons). These fields were generated by the interposition of paraffin layers with distinct thicknesses between the Am-Be source and the BF_3 detector. The BF_3 detector responses were recorded according to the number of paraffin planes used. MCNP simulations were also performed to study the detector responses on such experimental conditions. It has been possible to achieve the intended goal of evaluating the BF_3 detector response to different mixed irradiation fields.

1. INTRODUCTION

Boron Neutron Capture Therapy (BNCT) is a radio therapeutic procedure whose first proposition dates back to mid 1930's. In its earliest studies there were many difficulties which have not been overcome before the 1980's. When the international community became aware of the good results obtained by a Japanese group, BNCT felt a rebirth [1]. The BNCT enlarged its applications and much work has been done thereafter [2,3,4,5].
The treatment is based on two phases, the administration of a Boron compound to the patient that accumulates preferentially in tumor cells, and later the region that contains the cancerous tumor is irradiated with a thermal neutron flux [6].

When irradiated by thermal neutrons, the 10-B atom captures a neutron causing the following nuclear reactions [1]:

$$^{10}B + ^{1}n \rightarrow \left[^{11}B\right] \rightarrow ^{4}He + ^{7}Li + \gamma(0.48MeV) + 2.31MeV \qquad (94\%) \qquad (1)$$

$$^{10}B + ^{1}n \rightarrow \left[^{11}B\right] \rightarrow ^{4}He + ^{7}Li + 2.79MeV \qquad (6\%) \qquad (2)$$

The nuclear reaction products, ^{4}He and ^{7}Li, are ionizing particles with high linear energy transfer (LET), with an average range in tissue of approximately 9 μm for the alpha particle and 5 μm for lithium [1], which is the order of the dimensions of a human cell (10 μm). Therefore these particles loose their energy in nearby tumor cells.

Irradiation is done, in BNCT, with a neutron beam from a nuclear reactor, like the BNCT facility built at the IEA-R1 Reactor in IPEN/CNEN/SP [7]. For the use of this technique, it is necessary to know the thermal neutron flux [8] which reaches the tumor cells and also the intensity of the other components of the radiation field (fast neutrons and gamma radiation) [9]. Neutron flux measurements can be made by different techniques such as activation technique or through gas detectors like Boron Trifluoride detectors (BF_3).

The advantage of using a BF_3 detector over the activation technique is that it performs the measurements in real time. Besides its high sensitivity, this detector can work behind the shields and with small fields of thermal neutrons.

The BF_3 has high efficiency (greater than 90%) for thermal neutrons (with energy up to 0.5 eV) due to the presence of ^{10}B atoms in the detector [10]. The $^{10}B(n,\alpha)$ reaction has a cross section over thousand barns for thermal neutrons, while for fast neutrons, its value is much lower [11], as it is shown in Figure 1. So it is necessary to study the efficiency of these detectors when they are exposed to fields of different energies of neutrons (fast and epithermal). Despite the BF_3 detector is mostly sensitive to thermal neutrons, it is still sensitive to other neutron energy ranges. Simulations were run in order to evaluate the intensity of these contributions and to allow a better understanding of the data. Therefore, this work conducted a set of experiments and simulations, using MCNP [12], to evaluate the dependence of the efficiency of the BF_3 detectors with different neutron fields. Paraffin was used to decrease the neutron energy of these neutron fields. It was used due to its hydrogen abundance which presents high cross section to neutron elastic scattering (Figure 1).

The Monte Carlo method simulates a mathematical problem stochastically [13]. It has been often used to simulate processes involving random behavior and to quantify physical parameters that are difficult or even impossible to calculate by means of experimental measurements. Monte Carlo techniques have become popular in many areas, such as reactor physics and medical physics, due to the stochastic nature of radiation transport, emission and detection processes.

Therefore, the aim of this work is to study the efficiency of the detector BF_3 for thermal, epithermal and fast neutrons based on experiments and simulations results.

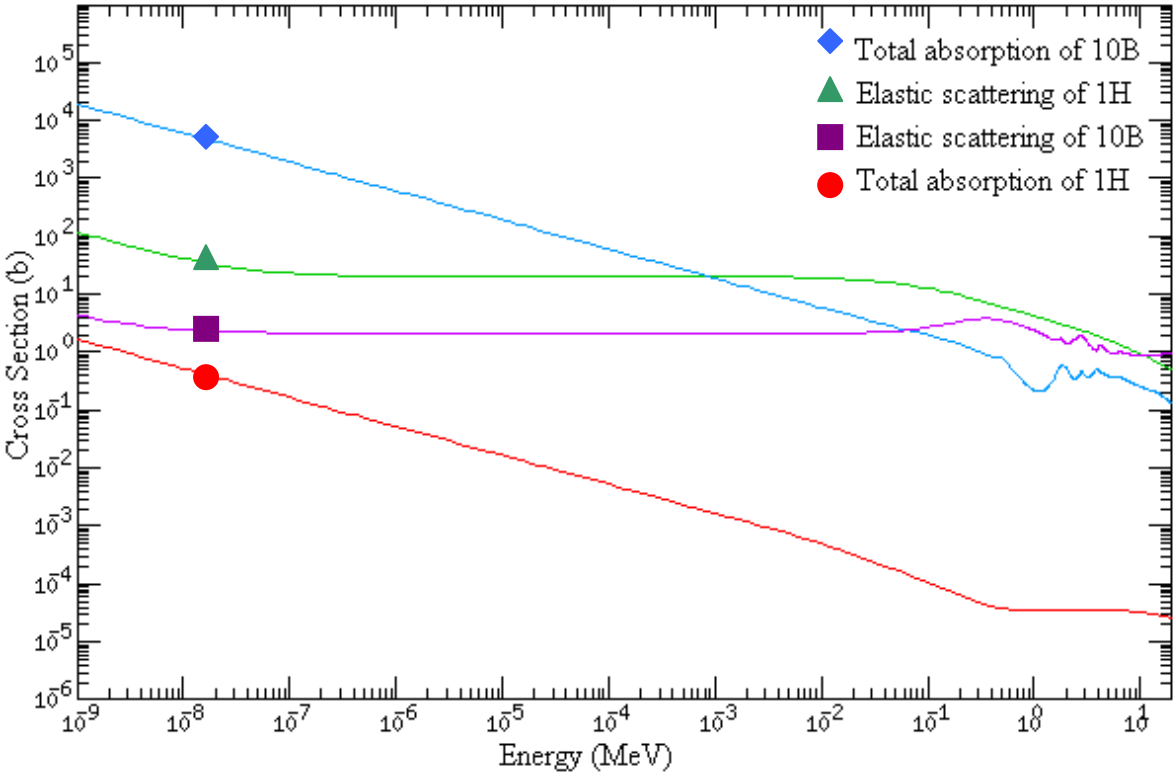

Figure 1. ^{1}H and ^{10}B neutron absorption and scattering cross sections [14].

2. MATERIALS AND METHODS

2.1. Experimental Setup

Thermal neutron flux impinging on the BF_3 detector was tallied for 14 distinct neutron fields. Neutron field changes were accomplished by interposing different amount of moderator between the neutron source and the detector.

The experiment consisted of a BF_3 detector with all associated electronic device, a Americium-Beryllium (Am-Be) source, 13 paraffin blocks (1x10x10 cm³) and 3 polyethylene blocks (6x30x35 cm³) used as shielding. For operation of the detector it was used a pre-amplifier model 142 coupled to the detector, it was also used an amplifier model 572 and a multichannel model 919 Spectrum Master to record the detector counting. All electronics used was produced by ORTEC.

The BF_3 detector used was the model S3179 from Reuter Stokes with 1.6 cm of diameter and 2.4 cm of active height, with sensitive volume of approximately 4.83 cm³.

The Am-Be source used is a cylindrical sealed source with 4.1 cm of height and 2.4 cm of diameter [15], 1 Ci of activity (^{241}Am), with a emission rate of $2.2x10^{6}$ neutrons per second [16]. Its neutron energy spectrum is shown in Figure 2.

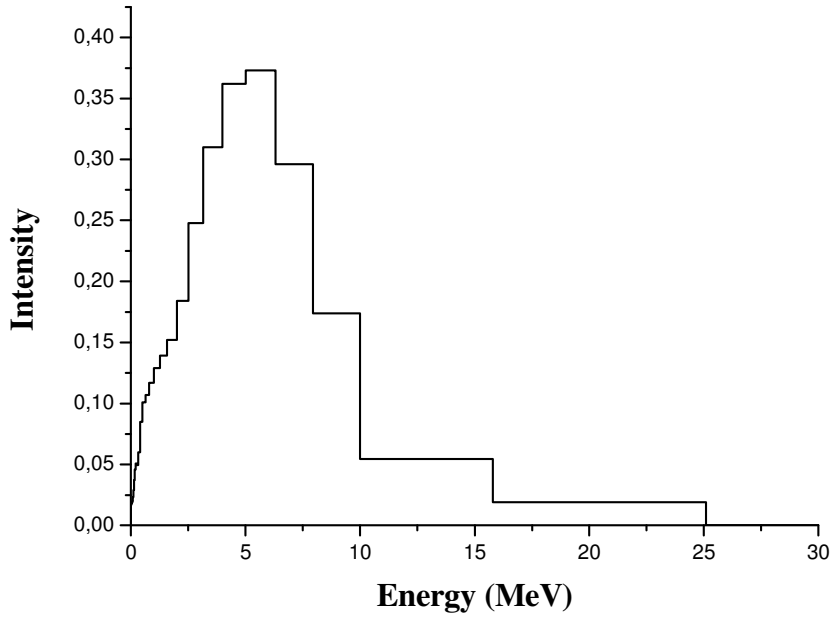

Figure 2. Am-Be neutron energy spectrum [17].

The Am-Be is a fast neutron source, which requires the use of moderators, such as paraffin, to slow the fast neutrons down to the thermal energy range. The paraffin layers were arranged by piling up a different number of 1 cm thick paraffin blocks. The BF_3 detector responses were recorded according to the number of paraffin blocks used.

A series of 1,000 s counts was performed starting from the detector direct exposition to the neutron source, i.e. with no paraffin blocks placed between them, followed by systematic addition of an extra paraffin block. The paraffin blocks slow the neutrons down changing the neutron energy spectrum of the neutron field at the detector location.

The experimental setup is shown in Figure 2. The BF_3 detector and the source of Am-Be were set 21.9 cm apart. The Am-Be was placed on a wooden table and the detector was held over the source by an Aluminum structure. Paraffin blocks were also hold over by this structure. Three polyethylene piles were placed on the table, around the experimental setup to stand as neutron shieldings.

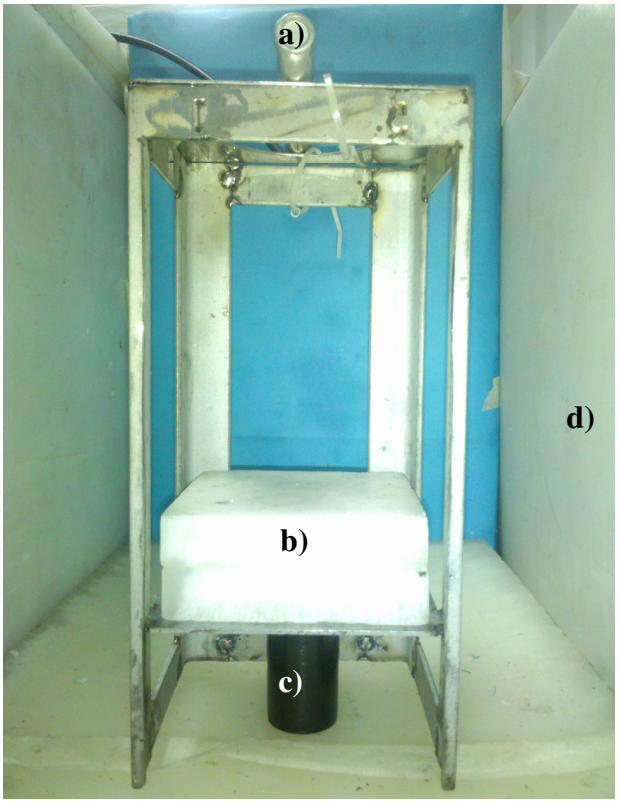

Figure 2. Experimental Setup: a) BF_3 detector; b) paraffin blocks; c) Am-Be source and d) polyethylene shielding.

2.2. MCNP Simulation

The experimental system was simulated with MCNP code [12]. This is a multi-purpose Monte Carlo based Radiation Transport code which simulates the interaction of radiation with matter.

The goal of the performed simulation, which reproduced the experiment realized in the laboratory, was to get a better and wider idea of the performed experiments. It provided complementary information which was either not accessed by the BF_3 detector, such as the dependence of the intensity of fast neutron flux on the number of paraffin blocks used, and/or reinforced the understanding of experiment.

Each component of the experiment was simulated (Figure 4). Neutron flux reaching the detector, splitted into 4 distinct energy components. Each simulation was run for 90 minutes which led to uncertainties lower than 2 %. ENDF/B-VI was used to provide the neutron cross section data needed to run MCNP calculations.

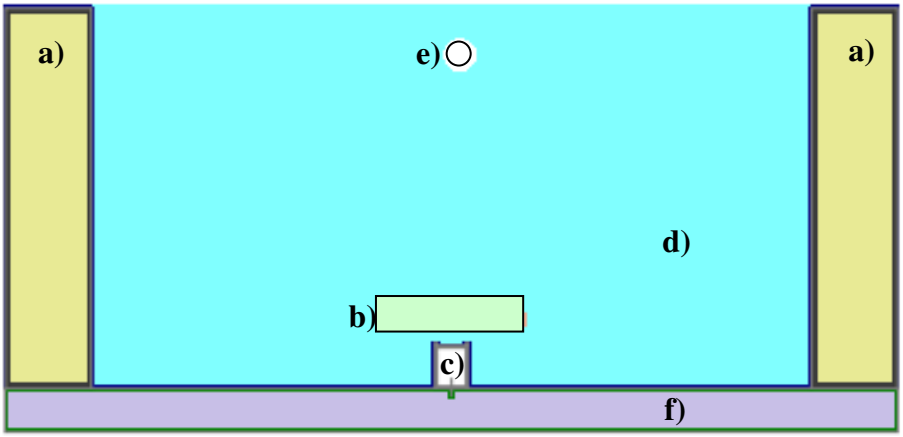

Figure 4. Simulated geometry: a) polyethylene shielding; b) paraffin block; c) Am-Be source, d) air, e) BF_3 detector and f) wooden table.

3. RESULTS

Through the experiment performed in the laboratory it was possible to measure the BF_3 detector countings when the blocks were inserted into the system. Figure 5 was generated by these data:

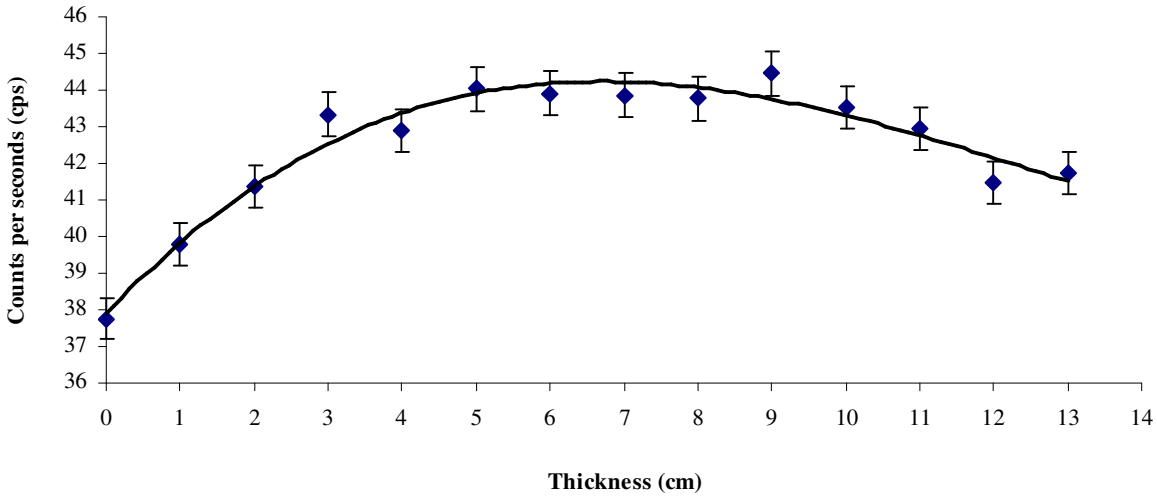

Figure 5. BF_3 counting rate versus paraffin thickness placed between the source and the detector.

Figure 5 shows an increase in the number of counting between 0 and 6 cm paraffin due to loss of fast and epithermal neutrons energy when they interact with the hydrogen atoms of the paraffin, becoming low energy neutrons and being more counted by the detector. Between 6 and 7 cm registered countings neither increase nor decrease, remaining constant. From 7 cm on there is a decrease in the recorded counting due to both the absorption of neutrons in the paraffin and the loss of some particles on their way to the detector, i.e. a large amount of neutrons are scattered away from the detector.

Although the AmBe is a fast neutron source, a large number of counts have been observed even before placing any paraffin block, (0 cm). These counting come from neutrons that have moderated by component systems other than paraffin, such as the wooden table and the polyethylene blocks. The fast neutrons interact with these components, lose some of their energy and are scattered. Some of these neutrons reach the detector, contributing for the observed counting for the no paraffin block configuration.

As the fast neutrons produced by the source go through the paraffin blocks, they lose energy by interaction with the hydrogen atoms of the paraffin and become low energy neutrons. The obtainment of thermal neutrons occurs due to the deceleration of fast neutrons, which lose some of their energy due to collision with heavy and medium nuclei by inelastic collisions and with light nuclei by elastic collisions [18].

MCNP simulations retrieved results which were not attained by the experiment. These simulated data provided a better insight of the carried experiment. It also helped to understand the role played by the different system components on the experimental data, standing as an essential tool on the BF_3 efficiency study. One set of the simulated data is shown in figure 6, just below. This figure shows the neutron fluxes dependence on the paraffin thickness placed between the source and the detector.

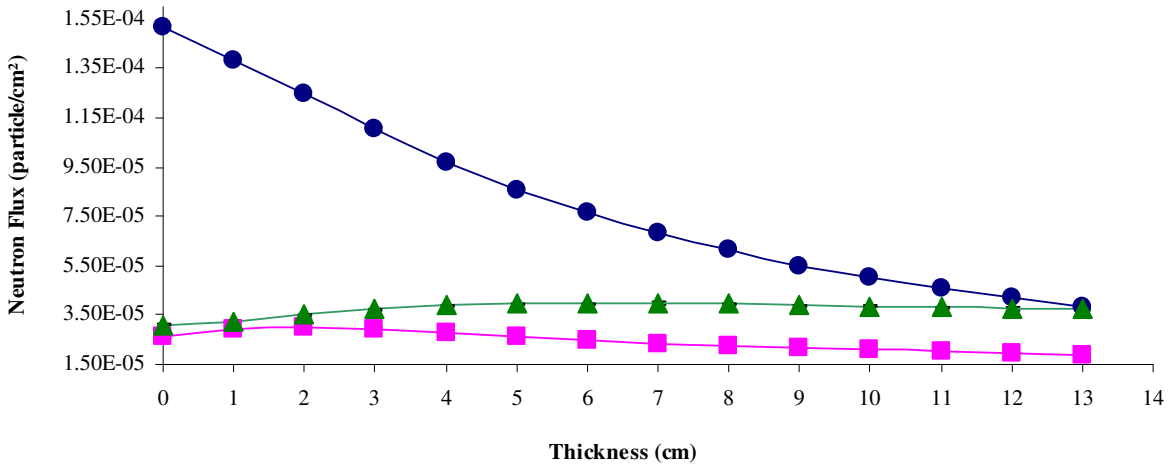

Figure 6. Simulated neutron fluxes versus paraffin thickness. circle, fast neutrons; square, epithermal neutrons; triangle, thermal neutrons. Statistical uncertainties are lower than 2 %.

One can see the changes on both neutron spectra and neutron field intensity with the addition of paraffin blocks. It is possible to verify that as the number of paraffin blocks increases the fast neutron flux decreases. The fast neutrons are slowed down to energies of the order ~0.025 eV through multiple scattering events with the hydrogen in the paraffin blocks [11].

It is also possible to verify in Figure 6 that between 0 and 2 cm of paraffin was observed an increase in the epithermal and thermal neutrons flux as the energy of fast neutrons decreases. For larger thickness of paraffin (2 – 6 cm) the thermal neutron flux is still increasing with decreasing of fast neutrons energy and to the same thickness range the epithermal neutron flux begins to decrease. Between 6 and 13 cm of paraffin was observed that the fast and epithermal neutrons flux continues to decrease and thermal neutron flux begins to fall.

Figure 7 depicts the thermal neutron flux profile shown above in a smaller scale.

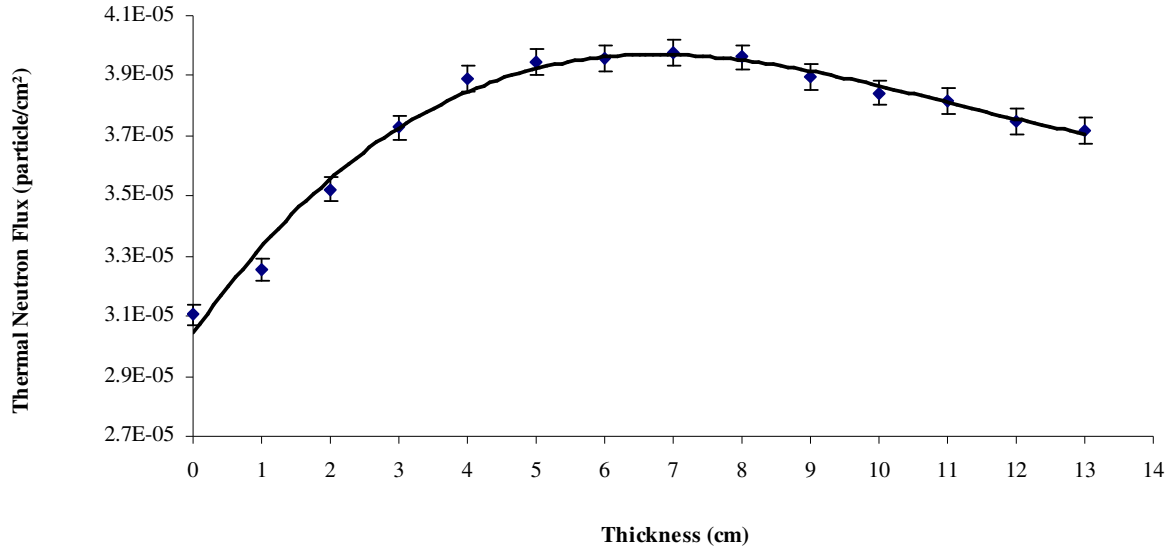

Figure 7. Simulateed thermal neutron flux versus paraffin thickness. Statistical uncertainties are lower than 2 %.

In Figure 7 it was also verified that between approximately 0 and 6 cm of paraffin occurs an increase production of particles in the thermal neutrons flux, thus increasing the thermal neutron flux when the fast and epithermal neutron flux decrease.

It is also possible to verify that for no paraffin blocks occurs a counting and this happens in the experimental part too. Because the interactions of neutrons with the others components of the system suffer scattering, reaching the detector.

So increasing the number of paraffin blocks (7 – 13 cm), more interactions occurs decreasing the neutron energy. Besides the neutrons loose energy when they interact with the paraffin

blocks, there is also scattering of neutrons, reducing more energy and so a small number of neutrons reach the detector.

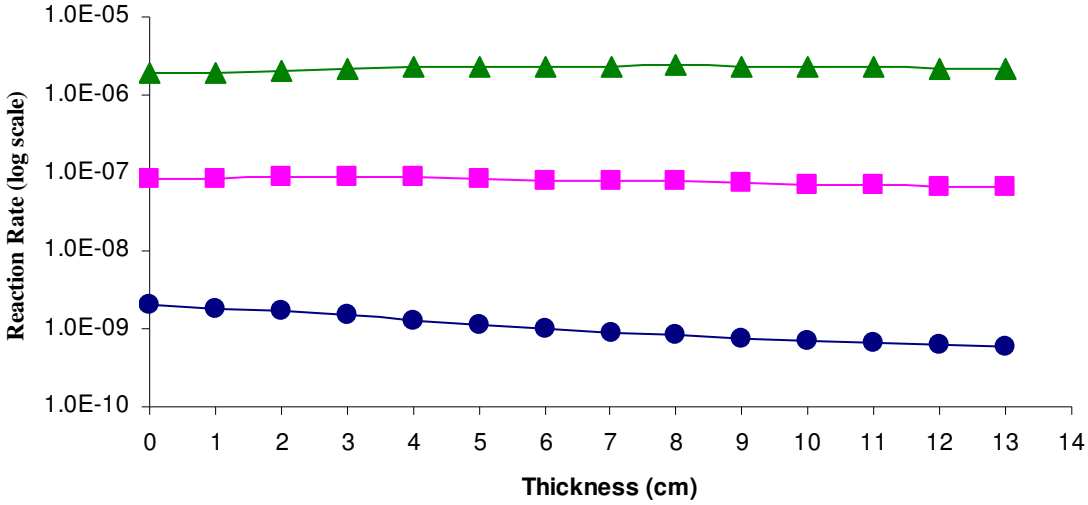

Figure 8. Simulated reaction rate, for 3 neutron energy ranges, versus paraffin thickness. Circle, fast neutrons; square, epithermal neutrons and triangle, neutrons. Statistical uncertainties are lower than 2 %.

With the simulation it was also possible to analyze the reaction rate for fast, epithermal and thermal neutrons fluxes (Figure 8). It was verified that order of size of the reaction rate varied from 10^{-9} to 10^{-7} to fast and epithermal neutrons and to thermal neutrons was over 10^{-6}, showing that the BF_3 detector respond mostly to thermal neutrons.

It is clear that the reaction rate for thermal neutrons is higher, but one can also notice that the detector is influenced by others field components, i.e. by neutrons from higher energy ranges. The contributions of epithermal and fast neutron to the detector efficiency are respectively 1 to 3 orders of magnitude lower. The observed fast neutron relative reduction to the detector efficiency comes from the fast neutrons flux decrease at the detector, as already shown in figure 6.

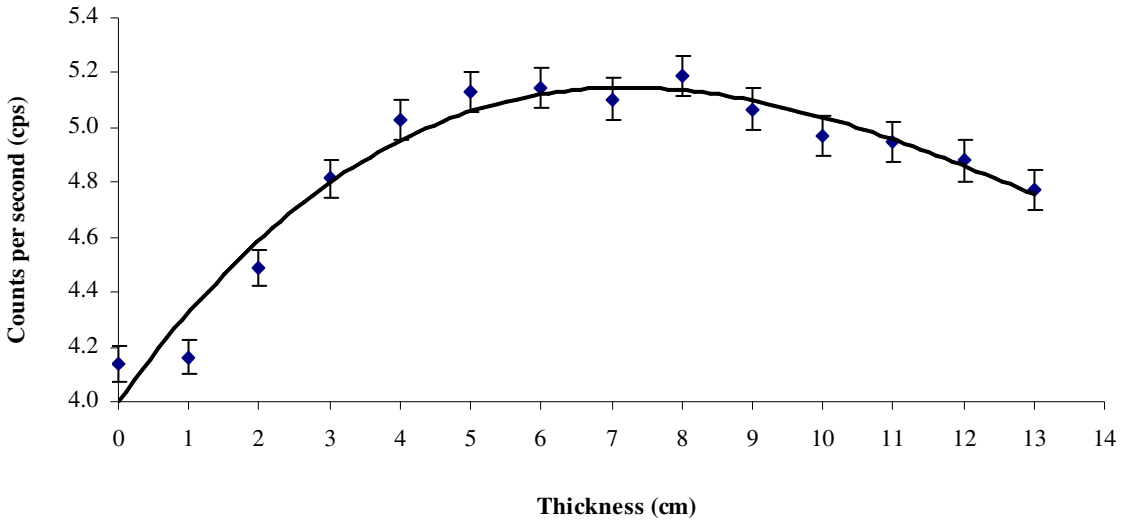

Figure 9. Simulated $^{10}B(n,\alpha)^{7}Li$ reaction rate in the BF3 detector versus paraffin thickness.

In Figure 9 it is shown the simulated $^{10}B(n,\alpha)^{7}Li$ reaction rate in the BF_3 detector dependence on the number of paraffin blocks inserted. For obtaining these values, the reaction rate values for thermal neutrons retrieved from simulation were multiplied by the Am-Be source neutron emission rate.

Comparing the experimental (Figure 5) and simulated (Figure 9) results, it is possible to observe a difference in order of size about 10. When the BF_3 detector was simulated, it was defined the characteristics of the same, as the active volume (4.8 cm³), density (2.76 mg.cm^{-3}) and gas pressure (55 cm Hg), but it may be that the active volume is greater than what was simulated, or even that the gas pressure is another and this contributes to the difference in order of size between the experimental and simulated results.

Both the experiment and the simulations reached the 13 cm of paraffin, if there were more paraffin blocks it would be possible to verify the absorption and scattering of neutrons, where they can no longer reach the detector due to low energy and the large number of interactions during the course of neutrons to the detector. For fast neutrons, many reactions are possible, but for thermal neutrons is capture the main cause of their removal from the beam [7].

4. DISCUSSIONS

In the experimental part carried was verified the highest amount of particles in the energy of thermal neutrons occurred between approximately 6 and 8 cm of paraffin (Figure 5). In the simulation performed the largest amount of particles (with energy of thermal neutrons) was reached in approximately 6.5 cm of paraffin (Figure 9).

There is a hypothesis that something has interfered with the experimental results compared with simulated, the experimental procedure to put up a paraffin block on the other, the two

blocks are not completely adhered, leaving between them air bubbles which could be interfering in the results. Already the simulations paraffin blocks adhere perfectly not letting the air interfere in the result.

On the efficiency of the BF_3 detector was possible to conclude with an analysis of counts in the experimental curve (Figure 5) and the simulated thermal neutron flux curve (Figure 7), that they have the same shape and therefore the efficiency of the detector is better for thermal neutrons. This type of detector has good efficiency for low energy neutron where the cross section of ^{10}B is high making the detector counting more, contrary to what happens with high energies where the cross section decreases which can be checked on Figure 1. And analyzing the curve of simulates reaction rate versus paraffin thickness (Figure 8) it is possible to conclude that the BF_3 detector was also influenced by other neutron field but on a small scale and that the BF_3 detector has higher reaction rate for thermal neutrons than for fast and epithermal neutrons, it shows the highest sensitivity of the detector for these neutrons and also shows why the detector has high efficiency for thermal neutrons.

In the curve of variation of neutron flux (Figure 6) there is an increase of thermal neutrons flux when paraffin blocks are inserted, where fast neutrons are thermalized loosing some of their energy and thus becoming low energy neutrons, which are detected by BF_3 detector. After reaching the highest thermal neutron flux and adding more paraffin blocks, thermal neutrons are scattered decreasing the thermal neutrons flux.

With the curve of simulates counting per second for thermal neutrons (Figure 9) it is possible to conclude that the characteristics of the detector were not correctly simulated, it must be simulated the active volume size of the detector and gas pressure for that the experiment can be simulated again and so the values of experimentally counting and simulated counting are the same order of size.

5. CONCLUSIONS

This work comprised the performance of both experiment and simulations and allowed the verification of several factors that influence the detection of neutrons by a BF_3 gas detector. Work can still be done on its improvement. It is possible to vary the gas detector used for further study of new neutron detectors and their efficiency. It is also possible to evaluate the influence of objects near the radioactive source and elaborate a experimental set up which most reinforces the event under study.

Simulations were meant to represent the closest possible the experiment conducted in the laboratory and thus verify the efficiency of the BF_3 detector analyzing the fast, epithermal and thermal neutron fluxes, reaction rates and counting of detector. With the simulation results it was possible to do a better analysis of the experimental data and get better comprehension about what happened in the experiment. It was possible to verify other factors that influenced the results, factors that might not be attained experimentally. Therefore, with the simulations, it was possible get better answers about how radiation interacted with each component of the experimental set up and how this influenced the results. However, if the geometries and the densities of each simulated material are not similar to the experimental procedure, the results may be different from the results obtained in the laboratory. The closer the simulation represents the experiment, the better the results.

The aim of this work was to study the efficiency of the BF_3 detector for different neutron energies and this goal was achieved. It was possible to analyze the efficiency of the detector and verify that some components used in the experiment and the simulations had a great influence on the results.

ACKNOWLEDGMENTS

The authors acknowledge CNPq for partial financial support.

REFERENCES

1. W. H. Sweet, "Early History of Development of Boron Neutron Capture Therapy of Tumors", *Journal of Neuro-Oncology*, **33**, pp. 19-26 (1997).
2. R. F. Barth, J.A.Coderre, M. Graça H. Vicente and T. E. Blue, "Boron Neutron Capture Therapy of Cancer: Current Status and Future Prospects", Clin Cancer Res. Journal, pp. 3987-4002 (2005).
3. F. Rahmani, M. Shahriari, A. Minoochchehr and H. Nedaie, "Feasibility study on the use of uranium in photoneutron target and BSA optimization for Linac based BNCT", Nuclear Instruments and Methods in Physics Research A, pp. 136-140 (2011).
4. E.C.C. Pozzi, S. Thorp, J. Brockman, M Miller, D. W. Nigg and M. F. Hawthorne, "Intercalibration of Physical Neutron Dosimetry for the RA-3 and MURR Thermal Neutron Sources for BNCT Small-Animal Research", 14th International Congress on Neutron Capture Therapy, pp. 402-405 (2010).
5. P. Tsai, Y. Liu, H. Liu and S. Jiang, "Characterization of a BNCT beam using neutron activation and indirect neutron radiography", Radiation Measurements, pp. 1167-1170 (2010).
6. R. F. Barth, A. H. Soloway and R. G. Fairchild, "Boron Neutron Capture Therapy for Cancer", *Scientific American*, pp.68-72 (1990).
7. P. R. P. Coelho, M. A. P. Camillo, M. A. Damy, D. B. M. Ferreira Jr., J. R. Maiorino, R. N. Mesquita, N. Nascimento, R. Pugliesi, J. R. Rogero, W. j. Vieira and G. S. Zahn, "Design of a Facility for NCT Research in the IEA-R1 Reactor", Advances in Neutron Capture Therapy, **1**, pp. 367-369 (1997).
8. P. R. P. Coelho, R. O. R. Muniz, J. F. Nascimento, G. S. A. e Silva, P. T. D Siqueira, H. Yoriyaz and V. Carneiro Jr., "Radiation Field Characterization of the NCT Research Facility at IEA-R1", 13th International Congress on Neutron Capture Therapy, **1**, pp. 553–555 (2008).
9. R. L. Moss, O. Aizawa, D. Beynon, R. Brugger, G. Constantine, O. Harling, H. B. Liu and P. Watkins, "The requirements and development of neutron beams for neutron capture therapy of brain cancer", *Journal of Neuro-Oncology*, **33**, pp.27-40 (1997).
10. G. F. Knoll, "*Radiation Detection and Measurement*", John Wiley & Sons, Inc., New York (2000).
11. E. Suckling, "Neutron Detection and Spectroscopy," University of Surrey, Guildford (2005).
12. F. Briesmeister, MCNP - A general Monte Carlo N-particle transport code, version 4C, Los Alamos National Laboratory, LA-13709-M, (April, 2000).

13. H. Yoriyaz, “Monte Carlo method: Principles and Applications in Medical Physics”, Revista Brasileira de Física Médica, **3**, pp.141-149 (2009).
14. Nuclear Data Evaluation Lab., accessed in July 22, 2011, http://atom.kaeri.re.kr/cgi-bin/endfform.pl.
15. T. M. Filho, “Desenvolvimento de Detector de Nêutrons usando sensor tipo barreira de superfície com conversor (n,p) e conversor (n,a)”, CNEN-IPEN, São Paulo (1999).
16. The Radiochemical Center Amersham, "Radiation sources, industrial and laboratory" (1977/8).
17. International Atomic Energy Agency, "Compendium of Neutron Spectra and Detector Responses for Radiation Protection Purpose", Vienna (2001).
18. C. B. Zamboni, "*Fundamentos da Física de Nêutrons*", Editora Livraria da Física, São Paulo (2007).